

Dwell time distributions for kinesin's mechanical steps

A. VALLERIANI^(a), S. LIEPELT and R. LIPOWSKY

Max Planck Institute of Colloids and Interfaces, Department of Theory & Bio-Systems - 14424 Potsdam, Germany, EU

received 14 January 2008; accepted in final form 5 March 2008
published online 11 April 2008

PACS 87.16.Nn – Motor proteins (myosin, kinesin dynein)

PACS 82.39.-k – Chemical kinetics in biological systems

PACS 87.16.Uv – Active transport processes

Abstract – The mechanical steps of molecular motors that walk processively along filaments are governed by four distinct dwell time distributions corresponding to the four possible pairs of subsequent forward and backward steps. These distributions can be calculated from the master equation for the network of motor states if one extends this network by two absorbing states and determines the corresponding absorption times. This procedure is illustrated for the kinesin motor for which the four dwell time distributions are explicitly calculated. The tails of these distributions are governed by a single decay rate Ω_1 , which corresponds to the smallest nonzero eigenvalue of the master equation. For kinesin, this theoretical decay rate is found to be in good agreement with the experimental rate Ω_{ex} as deduced from recent measurements.

Copyright © EPLA, 2008

Introduction. – Many molecular motors in the living cell transduce the chemical energy released from ATP hydrolysis into mechanical work [1]. A prominent example is provided by conventional kinesin [2,3], a molecular motor that walks processively along microtubules and is essential for intracellular transport and pattern formation. Kinesin has two identical motor heads and walks in a “hand-over-hand” fashion, *i.e.*, by alternating steps in which one head moves forward while the other one remains bound to the filament [4,5]. Each step leads to a motor displacement of 8 nm corresponding to the lattice constant of the microtubule. These mechanical steps are rather fast and completed within 15 microseconds [6].

Kinesin exhibits tight coupling, *i.e.*, it hydrolyzes one ATP molecule per mechanical step [7]. After ATP has been hydrolyzed by one of the catalytic motor domains, the inorganic phosphate is released rather fast, and both transitions together take of the order of 10 milliseconds to be completed [8]. ADP is subsequently released from the catalytic domain, and this release process is also completed during about 10 milliseconds [9]. When the catalytic domain of one motor head is occupied by ADP, this head is only loosely bound to the microtubule [10,11] and most likely to unbind from it. Various motor properties such as motor velocity [6,12], bound state diffusion coefficient (or randomness parameter) [12], ratio of forward to backward

steps [6], and run length [13] were measured as a function of ATP concentration and load force. Furthermore, the motor velocity was also determined as a function of P and ADP concentration [14].

As shown in [15–17], all of these experimentally observed motor properties can be described quantitatively within a recently introduced network model for the chemomechanical coupling of kinesin. In the present paper, we will use this model in order to calculate the dwell time distributions for kinesin's steps. We will start from the network of chemical states and “project” the corresponding network dynamics onto an effective step dynamics. The latter dynamics is non-Markovian and based on *conditional* mechanical steps or co-steps. In fact, one has four different co-steps that correspond to forward-after-forward steps, forward-after-backward steps, backward-after-forward steps, and backward-after-backward steps. Each of these co-steps is characterized by its own dwell time distribution. Thus, the effective step dynamics is governed by four different dwell time distributions.

Our letter is organized as follows. First, we give a precise definition for the co-step dynamics which leads to an extended network with two absorbing states. We then use the general formalism for continuous-time Markov chains with absorbing states to calculate the dwell time distributions for the four distinct co-steps. Finally, we relate these distributions to the ones observed experimentally in [6].

^(a)E-mail: valleriani@mpikg.mpg.de

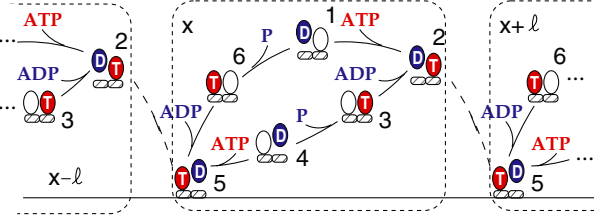


Fig. 1: Network representation for the kinesin motor [15,16] with six chemical states labeled by $i = 1, 2, \dots, 6$ that are distinguished by the chemical composition of the two catalytic motor domains. A transition from state i to state j is denoted by $|ij\rangle$. An edge between two states i and j represents both the forward transition $|ij\rangle$ and the backward transition $|ji\rangle$; a solid and broken edge corresponds to a pair of chemical and mechanical transitions, respectively. The horizontal line at the bottom represents the filament which provides a discrete set of binding sites at the spatial positions $x \pm n\ell$ with $n = 0, 1, \dots$.

As a result, we find good agreement between theory and experiment without adjusting any model parameter.

Dynamics of co-steps. – As explained in [16], the kinesin motor can be described, for small ADP concentration, by the 6-state network shown in fig. 1. In this figure, we have explicitly included the spatial coordinate x parallel to the filament by replicating the network in a periodic manner. The periodicity is provided by the mechanical step size, ℓ , for the center-of-mass displacement of the motor. A motor is in state i_x when its chemical state is i and its spatial position is x . By convention, the transition $|2_x 5_{x+\ell}\rangle$ from state 2_x to state $5_{x+\ell}$ represents a *forward* mechanical transition, whereas the transition, $|5_{x+\ell} 2_x\rangle$ represents a *backward* mechanical transition.

With a forward mechanical transition the motor completes a forward step, whereas with a backward mechanical transition the motor completes a backward step. Indeed, inspection of fig. 1 shows that the motor attains the chemical state $i = 5$ immediately after a forward step and the chemical state $i = 2$ immediately after a backward step. It may then undergo an arbitrary number of chemical transitions before it performs another mechanical transition in the forward or backward direction. Thus, if we focus on the step mechanics, we must distinguish four co-steps, denoted by σ_{ff} , σ_{fb} , σ_{bf} , and σ_{bb} , corresponding to i) a forward after a forward, ii) a backward after a forward, iii) a forward after a backward, and iv) a backward after a backward step, respectively.

As an example, let us consider a co-step σ_{ff} . Any such co-step corresponds to a network walk with the following properties: i) The walk starts from the initial state 5_x and ends up in the final state $5_{x+\ell}$; and ii) the walk may contain an arbitrary number of chemical transitions but must contain only one mechanical transition given by $|2_x 5_{x+\ell}\rangle$, which is, in fact, the final transition of this walk. We will denote such a walk by $|5_x \rightarrow 5_{x+\ell}\rangle$. Likewise, the

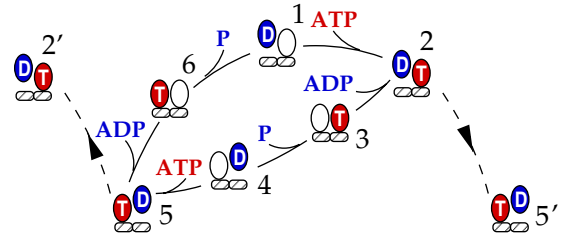


Fig. 2: Extended (6+2)-state network for kinesin which consists of the six chemical states as in fig. 1 together with the two absorbing states $2'$ and $5'$.

co-steps σ_{ff} , σ_{bf} , and σ_{bb} correspond to walks $|5_x \rightarrow 2_{x-\ell}\rangle$, $|2_x \rightarrow 5_{x+\ell}\rangle$, and $|2_x \rightarrow 2_{x-\ell}\rangle$, respectively.

All walks that contribute to any of the four co-steps are distinguished by the property that they leave the chemical network at x only once, either towards the final state $5_{x+\ell}$ or towards the final state $2_{x-\ell}$. These two final states thus represent two absorbing states $5'$ and $2'$ which lead to the extended (6+2)-state network shown in fig. 2. The four co-steps are now provided by walks that start in the initial states $i = 2$ or $i = 5$ and end in the final states $j = 5'$ or $j = 2'$ and, thus, are described by

$$\begin{aligned} \sigma_{ff} &= |5 \rightarrow 5'\rangle, & \sigma_{bf} &= |2 \rightarrow 5'\rangle, \\ \sigma_{fb} &= |5 \rightarrow 2'\rangle, \text{ and} & \sigma_{bb} &= |2 \rightarrow 2'\rangle. \end{aligned} \quad (1)$$

Furthermore, the dwell times t_{ff} , t_{bf} , t_{fb} and t_{bb} for the different co-steps are now equivalent to the absorption times of the corresponding walks on the extended (6+2)-state network in fig. 2.

Each dwell time t_α with $\alpha = ff, fb, bf$ or bb is governed by the probability distribution $\rho_\alpha(t)$ which determines the probability

$$\Pr\{t_\alpha \leq t\} = \int_0^t du \rho_\alpha(u), \quad (2)$$

and the average dwell time τ_α .

Markov chains with absorbing states. – To compute the probability distributions of the dwell times, we now introduce some formalism for Markov chains. Let $X(t)$ with time $t \geq 0$ be a continuous-time Markov chain that can attain $N+1$ discrete states $i = 0, 1, \dots, n-1, n, \dots, N$, where the first n states $\{0, 1, \dots, n-1\}$ are transient states and the remaining $N+1-n$ states $\{n, \dots, N\}$ are absorbing states. The conditional probabilities that the process dwells in state j at time t provided it started in the initial state i at time $t=0$, are denoted by

$$P_{ij}(t) = \Pr\{X(t) = j | X(0) = i\}. \quad (3)$$

When the process dwells in state i , it undergoes a transition to state j with transition rate $\omega_{ij} \geq 0$. The time evolution of the probabilities $P_{ij}(t)$ is then governed by

the master equation

$$\dot{P}_{ij} \equiv \frac{d}{dt} P_{ij} = \sum_{k \neq j} [P_{ik}(t) \omega_{kj} - P_{ij}(t) \omega_{jk}] \quad (4)$$

with $P_{ii}(0) = 1$ and $\sum_j P_{ij}(t) = 1$. This equation has a steady-state solution, P_{ij}^{st} . Obviously, $P_{ij}^{\text{st}} = 0$ for any transient state j , and $\sum_{k=n}^N P_{ik}^{\text{st}} = 1$. Thus, starting in the initial transient state i with $0 \leq i < n-1$, the probability that the walk is absorbed in state k with $n \leq k \leq N$ is given by

$$A_{ik} \equiv P_{ik}^{\text{st}} = \Pr\{X^{\text{ab}} = k | X(0) = i\}. \quad (5)$$

Here and below, the superscript “ab” stands for “absorption”. Furthermore, the probability $P_{ij,k}(t)$ that the process starts in state i , sojourns in state j at time t , and is eventually absorbed in state k , can be expressed as

$$\begin{aligned} P_{ij,k}(t) &= \Pr\{X(t) = j, X^{\text{ab}} = k | X(0) = i\} \\ &= P_{ij}(t) A_{jk}. \end{aligned} \quad (6)$$

On every transient state i , the process will sojourn for an exponentially distributed random time with rate $\sum_{j=0}^N \omega_{ij}$ and will then jump to a neighboring state j with probability $\omega_{ij} / \sum_j \omega_{ij}$. This jump process will continue until an absorbing state is reached. The absorption time, $t_i^{\text{ab}} \geq 0$, is then defined via

$$t_i^{\text{ab}} = \min \{t \geq 0, X(t) = k \geq n | X(0) = i\}, \quad (7)$$

i.e., the time required to reach any absorbing state from the initial state $X(0) = i$. The probability that the absorption time $t_i^{\text{ab}} \leq t$ can be expressed as

$$\Pr\{t_i^{\text{ab}} \leq t\} = \sum_{k=n}^N P_{ik}(t) \equiv \int_0^t du \rho_i^{\text{ab}}(u), \quad (8)$$

with the probability distribution

$$\rho_i^{\text{ab}}(t) = \sum_{k=n}^N \dot{P}_{ik}(t), \quad (9)$$

a relation that was also derived recently in [18]. The average absorption time starting from the transient state i is now denoted by τ_i^{ab} .

Conditional absorption times. – In the previous subsection, we considered all possible walks of the Markov process. Now, we want to focus on the subset of those walks that are eventually absorbed in a certain state k . Thus, we now consider the conditional probabilities

$$P_{ij|k}(t) = \Pr\{X(t) = j | X(0) = i, X^{\text{ab}} = k\}, \quad (10)$$

with $i \leq n-1$ and $k \geq n$. Since a walk that starts from state i is absorbed in state k with absorption probability A_{ik} , see (5), the conditional probability $P_{ij|k}$ is given by

$$P_{ij|k}(t) = P_{ij,k}(t) / A_{ik} = P_{ij}(t) A_{jk} / A_{ik}, \quad (11)$$

where the first equality arises after re-arranging the terms in the conditional probability (10). The conditional

probabilities $P_{ij|k}(t)$ describe the time evolution on the restricted Markov chain with n transient states as before but with only one absorbing state, namely k . The corresponding absorption times $t_{i|k}^{\text{ab}}$ satisfy

$$\Pr\{t_{i|k}^{\text{ab}} \leq t\} = P_{ik|k}(t) \equiv \int_0^t du \rho_{i|k}^{\text{ab}}(u), \quad (12)$$

which defines the probability distribution $\rho_{i|k}^{\text{ab}}$ for the restricted process. Finally, it follows from the transformation rule (11) and $A_{kk} = 1$ that

$$\rho_{i|k}^{\text{ab}}(t) = \dot{P}_{ik|k}(t) = \dot{P}_{ik}(t) / A_{ik}. \quad (13)$$

Relation (13) was previously stated in refs. [19,20] for a generic birth and death process. We will denote the average absorption time corresponding to the conditional probability distribution (13) by $\tau_{i|k}^{\text{ab}}$.

Using the general properties of Markov processes with absorbing states as discussed in the previous sections, we can now compute the probability distributions for kinesin's co-steps σ_α with $\alpha = \text{ff}, \text{fb}, \text{bf}$ or bb as in (1), see also fig. 2. Alternatively, both the absorption probabilities A_{ik} and the average absorption times $\tau_{i|k}^a$ can be computed via another algebraic approach that is based on the transformation rule (11) and matrix algebra rather than on integration of the master equation [21]. We have used this algebraic approach to check some of our results. In addition, we also performed stochastic simulations based on the Gillespie algorithm to directly compute the probability distributions and all other quantities discussed here.

Transition rates for kinesin. – After this general discussion of Markov processes with absorption, we now return to our specific Markov process for the molecular-motor kinesin, which corresponds to the extended (6+2)-network in fig. 2. In the latter network, the states $i = 5, 6, 1, 2, 3$, and 4 are transient, the states $k = 5'$ and $2'$ are absorbing.

For the network shown in fig. 2, the transition rates ω_{ij} depend on several thermodynamic control parameters, namely the external load force F and the concentrations [ATP], [ADP], and [P]. These functional dependences have been determined previously in [16] i) by comparing the steady-state properties of the chemomechanical network of motor states with the available experimental data from single-molecule experiments and ii) by imposing energy (or steady-state) balance conditions that represent general thermodynamic constraints on the transition rates. This matching procedure, the details of which are explained in [16], leads to the transition rates ω_{ij} as given in table 1. Inspection of this table shows that all rates depend on the dimensionless force

$$F^* \equiv \ell F / k_B T \quad (14)$$

with the step size $\ell = 8 \text{ nm}$ and the thermal energy $k_B T = 4 \times 10^{-21} \text{ J}$ at room temperature. Furthermore, all transitions that involve the binding of a single molecule

Table 1: Transition rates ω_{ij} for the extended (6+2)-state network in fig. 2, which depend on the dimensionless load force F^* and the concentrations [ATP], [ADP], and [P]. The list of transition rates given in this table is complemented by the symmetry conditions $\omega_{23} = \omega_{56}$, $\omega_{34} = \omega_{61}$, $\omega_{45} = \omega_{12}$, $\omega_{32} = \omega_{65}$, and $\omega_{43} = \omega_{16}$. The concentrations are in units of μM , the rate constants in units of $1/\text{s}$ or $1/(\text{s } \mu\text{M})$.

$\omega_{56} = 200/(1 + \exp(0.15 F^*))$
$\omega_{61} = 200/(1 + \exp(0.15 F^*))$
$\omega_{12} = 4[\text{ATP}] / (1 + \exp(0.25 F^*))$
$\omega_{25'} = 2.9 \times 10^5 \exp(-0.65 F^*)$
$\omega_{65} = 0.1[\text{ADP}] / (1 + \exp(0.15 F^*))$
$\omega_{16} = 0.02[\text{P}] / (1 + \exp(0.15 F^*))$
$\omega_{21} = 200/(1 + \exp(0.25 F^*))$
$\omega_{52'} = 0.24 \exp(0.35 F^*)$
$\omega_{54} = 1.37 \times 10^{-10} / (1 + \exp(0.25 F^*))$

of ATP, ADP, or P, compare fig. 1, are proportional to [ATP], [ADP], or [P], respectively.

Statistics of kinesin's mechanical steps. – As previously mentioned, each co-step σ_α with $\alpha = \text{ff}, \text{fb}, \text{bf}$ or bb , corresponds to a walk that starts in either of the two initial states $i = 5$ or 2 and ends in either of the two absorbing states $k = 5'$ or $2'$. Thus, the absorption probabilities A_{ik} defined in (5) determine the transition probabilities M_α via

$$\begin{aligned} M_{\text{ff}} &= A_{55'} = P_{55'}^{\text{st}}, & M_{\text{bf}} &= A_{25'} = P_{25'}^{\text{st}}, \\ M_{\text{fb}} &= A_{52'} = P_{52'}^{\text{st}}, & M_{\text{bb}} &= A_{22'} = P_{22'}^{\text{st}}, \end{aligned} \quad (15)$$

with $M_{\text{ff}} + M_{\text{fb}} = 1$ and $M_{\text{bf}} + M_{\text{bb}} = 1$.

The transition probabilities M_α in (15) define a new discrete-time Markov chain that represents the random sequence of forward (f) and backward (b) steps of the motor. This new process is defined by the recursion relation

$$(\pi'_f, \pi'_b) = (\pi_f, \pi_b) \mathbf{M} \quad (16)$$

for the probabilities π_f and $\pi_b = 1 - \pi_f$ to make a forward and backward step, respectively, with the stochastic matrix

$$\mathbf{M} \equiv \begin{pmatrix} M_{\text{ff}} & M_{\text{fb}} \\ M_{\text{bf}} & M_{\text{bb}} \end{pmatrix}. \quad (17)$$

The steady state with $(\pi'_f, \pi'_b) = (\pi_f, \pi_b) = (\pi_f^{\text{st}}, \pi_b^{\text{st}})$ is given by

$$\begin{aligned} \pi_f^{\text{st}} &= M_{\text{bf}} / (M_{\text{bf}} + M_{\text{fb}}), \\ \pi_b^{\text{st}} &= M_{\text{fb}} / (M_{\text{bf}} + M_{\text{fb}}) = 1 - \pi_f^{\text{st}}, \end{aligned} \quad (18)$$

which implies the forward to backward step ratio

$$q = \pi_f^{\text{st}} / \pi_b^{\text{st}} = M_{\text{bf}} / M_{\text{fb}} = P_{25'}^{\text{st}} / P_{52'}^{\text{st}}. \quad (19)$$

The co-steps σ_α with $\alpha = \text{ff}, \text{fb}, \text{bf}$ or bb represent pairs of two subsequent events in the random sequence of f and b steps. It is not difficult to show that the steady-state

frequencies, π_α^{st} , of these four events are given by

$$\begin{aligned} \pi_{\text{ff}}^{\text{st}} &= \pi_f^{\text{st}} M_{\text{ff}}, & \pi_{\text{bf}}^{\text{st}} &= \pi_b^{\text{st}} M_{\text{bf}}, \\ \pi_{\text{fb}}^{\text{st}} &= \pi_f^{\text{st}} M_{\text{fb}}, & \pi_{\text{bb}}^{\text{st}} &= \pi_b^{\text{st}} M_{\text{bb}}, \end{aligned} \quad (20)$$

with the symmetry relation $\pi_{\text{bf}}^{\text{st}} = \pi_{\text{fb}}^{\text{st}}$ as follows from (18). Furthermore, the relations $M_{\text{ff}} + M_{\text{fb}} = 1$ and $M_{\text{bf}} + M_{\text{bb}} = 1$ imply $\pi_{\text{ff}}^{\text{st}} + \pi_{\text{bf}}^{\text{st}} = \pi_f^{\text{st}}$ and $\pi_{\text{fb}}^{\text{st}} + \pi_{\text{bb}}^{\text{st}} = \pi_b^{\text{st}}$ as well as

$$\pi_{\text{ff}}^{\text{st}} - \pi_{\text{bb}}^{\text{st}} = \pi_f^{\text{st}} - \pi_b^{\text{st}}. \quad (21)$$

Average dwell times for kinesin's co-steps. –

The average dwell times τ_α of the four co-steps, which have been introduced after (2), can be identified with the average absorption times $\tau_{i|k}^{\text{ab}}$ for the restricted processes that start in the initial states $i = 5$ or 2 and end up in the absorbing states $k = 5'$ or $2'$. The latter times have been defined after (13). In this way, we obtain the average dwell times

$$\begin{aligned} \tau_{\text{ff}} &= \tau_{5|5'}^{\text{ab}}, & \tau_{\text{bf}} &= \tau_{2|5'}^{\text{ab}}, \\ \tau_{\text{fb}} &= \tau_{5|2'}^{\text{ab}}, & \tau_{\text{bb}} &= \tau_{2|2'}^{\text{ab}}, \end{aligned} \quad (22)$$

for the four different co-steps. By averaging over the four co-steps, we obtain the average stepping time

$$\langle \tau \rangle = \sum_\alpha \pi_\alpha^{\text{st}} \tau_\alpha, \quad (23)$$

where the summation runs over $\alpha = \text{ff}, \text{fb}, \text{bf}$ and bb .

The average motor velocity v is then given by

$$v = (\pi_f^{\text{st}} - \pi_b^{\text{st}}) \ell / \langle \tau \rangle = (\pi_{\text{ff}}^{\text{st}} - \pi_{\text{bb}}^{\text{st}}) \ell / \langle \tau \rangle, \quad (24)$$

where ℓ denotes again the step size and relation (21) has been used.

Dependence on external load force. – The motor velocity v changes sign at the stall force $F = F_s = 7 \text{ pN}$ [6] which corresponds to the dimensionless stall force $F_s^* = 14$, compare (14). The force dependence of the steady-state probabilities π_α^{st} and the average dwell times τ_α is displayed in fig. 3(a) and (b), respectively. Inspection of this figure shows that the co-steps σ_{ff} and σ_{bb} dominate for forces $F^* \ll F_s^*$ and $F^* \gg F_s^*$, respectively. Close to the stall force F_s^* , the co-steps σ_{bf} and σ_{fb} , which do not lead to a net displacement of the motor, are most probable.

Thus, for small and large load forces, the motor makes primarily forward-after-forward steps and backward-after-backward steps, respectively, whereas it typically alternates between forward and backward steps close to the stall force.

On the other hand, the average dwell times τ_{ff} and τ_{bb} for the co-steps σ_{ff} and σ_{bb} are found to be equal for all values of the load force F^* as explained further below and to increase monotonically with increasing load F^* . This monotonic increase is consistent with the experimental observation in [6] that the backward velocity is rather small and decays to zero in the limit of large load forces.

Dwell time distributions of co-steps. – The probability distributions ρ_α of the dwell times t_α can be obtained

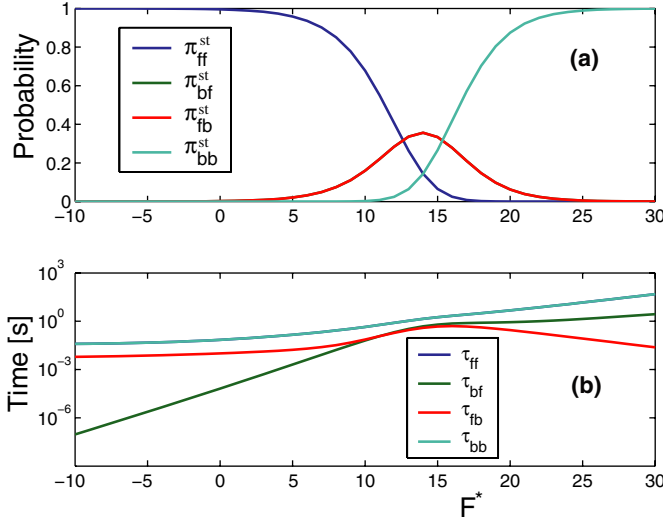


Fig. 3: (a) Steady-state probabilities π_{α}^{st} and (b) average dwell times τ_{α} computed via (20) and (22), respectively, as functions of the dimensionless load force F^* for $[\text{ATP}] = 10 \mu\text{M}$ and $[\text{ADP}] = [\text{P}] = 0.5 \mu\text{M}$. Note the semi-logarithmic scale in (b). In (a), the curve for $\pi_{\text{bf}}^{\text{st}}$ is covered by the curve for $\pi_{\text{fb}}^{\text{st}}$. In (b), the curve for τ_{ff} is covered by the curve for τ_{bb} .

from relation (13) which leads to

$$\rho_{\text{ff}}(t_{\text{ff}}) = \dot{P}_{55'}(t_{\text{ff}})/M_{\text{ff}} = \dot{P}_{55'}(t_{\text{ff}})/P_{55'}^{\text{st}}, \quad (25)$$

$$\rho_{\text{bf}}(t_{\text{bf}}) = \dot{P}_{25'}(t_{\text{bf}})/M_{\text{bf}} = \dot{P}_{25'}(t_{\text{bf}})/P_{25'}^{\text{st}}, \quad (26)$$

$$\rho_{\text{fb}}(t_{\text{fb}}) = \dot{P}_{52'}(t_{\text{fb}})/M_{\text{fb}} = \dot{P}_{52'}(t_{\text{fb}})/P_{52'}^{\text{st}}, \quad (27)$$

$$\rho_{\text{bb}}(t_{\text{bb}}) = \dot{P}_{22'}(t_{\text{bb}})/M_{\text{bb}} = \dot{P}_{22'}(t_{\text{bb}})/P_{22'}^{\text{st}}, \quad (28)$$

where the time derivatives on the right-hand side of these equations are obtained from the master equation (4) and the transition probabilities M_{α} have been defined in (15).

All four dwell time distributions as given by (25)–(28) are nonexponential as shown in fig. 4 and, thus, directly demonstrate the non-Markovian character of the mechanical stepping process. The dwell time distributions ρ_{ff} and ρ_{bb} for forward-after-forward and backward-after-backward steps as shown in fig. 4(a) and (d) decrease to zero for small dwell times since the motor has to visit at least two other motor states, namely $i = 1, 6$ or $i = 3, 4$, before he can make the next mechanical step, see fig. 2. On the other hand, the dwell time distributions ρ_{fb} and ρ_{bf} for forward-after-backward and for backward-after-forward steps as shown fig. 4(b) and (c) exhibit several characteristic time scales. These latter distributions always have a boundary maximum at vanishing dwell times corresponding to two subsequent mechanical transitions without any intervening chemical transition. However, with increasing load force, these distributions also develop a second shoulder at larger dwell times corresponding to cycles of intervening chemical transitions that start from state $i = 2$ or state $i = 5$ and return to the same state before making the next mechanical transition.

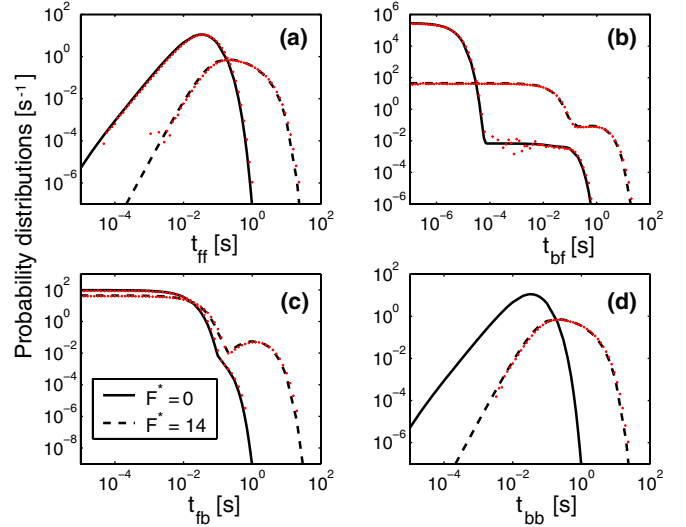


Fig. 4: Probability distributions ρ_{α} of the dwell times t_{α} for the four co-steps σ_{α} with $\alpha = \text{ff}, \text{fb}, \text{bf}$, and bb as computed via (25)–(28). The black solid and broken lines correspond to vanishing load force $F^* = 0$ and stall force $F^* = F_s^* = 14$, respectively, with $[\text{ATP}] = 10 \mu\text{M}$ and $[\text{ADP}] = [\text{P}] = 0.5 \mu\text{M}$. The red data points have been obtained by stochastic simulations of the stepping process using the Gillespie algorithm.

Comparison of fig. 4(a) and (d) also reveals that the two dwell time distributions $\rho_{\text{ff}}(t)$ and $\rho_{\text{bb}}(t)$ are, in fact, identical. This equality arises from the symmetry of the underlying transition rates ω_{ij} , see caption of table 1, which implies that the average sojourn times for the motor in the states 6 and 1 are equal to those on states 3 and 4, respectively. Similar symmetries have been found in other models of molecular motors as discussed in [20]. An immediate consequence of the equality $\rho_{\text{ff}}(t) = \rho_{\text{bb}}(t)$ for the dwell time distributions is the equality $\tau_{\text{ff}} = \tau_{\text{bb}}$ for the corresponding average dwell times as previously shown in fig. 3(b).

Comparison with experimental data. – Carter and Cross [6] have measured the probability distributions for forward and backward steps of kinesin. A forward step corresponds either to a co-step σ_{ff} or to a co-step σ_{bf} . Thus, the dwell time t_f of forward steps is governed by the probability distribution

$$\begin{aligned} \rho_f(t_f) &= (\pi_{\text{ff}}^{\text{st}}/\pi_f^{\text{st}}) \rho_{\text{ff}}(t_f) + (\pi_{\text{bf}}^{\text{st}}/\pi_f^{\text{st}}) \rho_{\text{bf}}(t_f) \\ &= \dot{P}_{55'}(t_f) + (1/q) \dot{P}_{25'}(t_f), \end{aligned} \quad (29)$$

where q is the forward to backward step ratio defined in (19). Likewise, the dwell time t_b of backward steps is distributed according to

$$\begin{aligned} \rho_b(t_b) &= (\pi_{\text{fb}}^{\text{st}}/\pi_b^{\text{st}}) \rho_{\text{fb}}(t_b) + (\pi_{\text{bb}}^{\text{st}}/\pi_b^{\text{st}}) \rho_{\text{bb}}(t_b) \\ &= q \dot{P}_{52'}(t_b) + \dot{P}_{22'}(t_b). \end{aligned} \quad (30)$$

The experimental data for the distributions $\rho_f(t_f)$ and $\rho_b(t_b)$ as obtained in [6] are restricted to dwell times

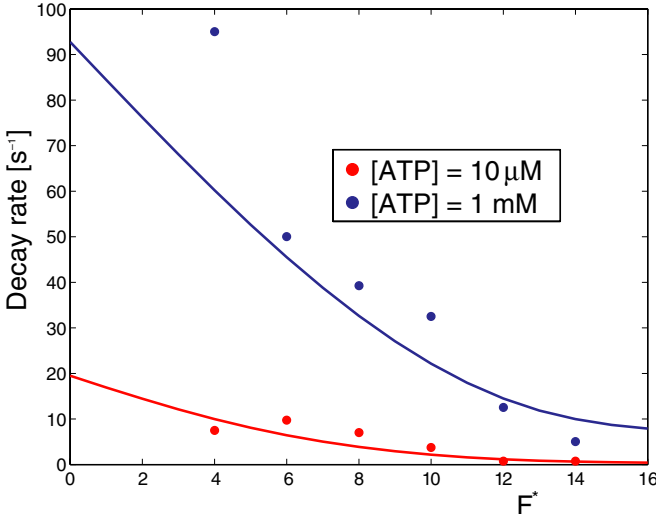


Fig. 5: Decay rates Ω_{ex} (data points) and Ω_1 (solid curves) for the tail of the dwell time distribution $\rho_f(t_f)$ as a function of dimensionless load force F^* for two values of ATP concentration. The theoretical rates Ω_1 follow from (29) with $[\text{ADP}] = [\text{P}] = 0.5 \mu\text{M}$ and correspond to the smallest nonzero eigenvalue of the master equation (4). The experimental rates Ω_{ex} have been obtained in [6].

that exceed a certain small time cutoff, t_{\min} , which varies between 0.01 and 0.1 s depending on ATP concentration and load force. For $t_f > t_{\min}$, the measured distributions $\rho_f(t_f)$ have been fitted to single exponential functions of the form $\rho_f(t) \sim \exp(-\Omega_{\text{ex}}t)$ which defines the decay rate Ω_{ex} . This experimentally determined rate depends on load force and ATP concentration as shown in fig. 5.

For comparison, fig. 5 also contains the decay rate Ω_1 as obtained from our theory for the tails of the dwell time distributions $\rho_f(t_f)$ and $\rho_b(t_b)$. The decay rate Ω_1 corresponds to the smallest nonzero eigenvalue of the master equation (4). In general, this latter equation has a discrete spectrum of nonzero eigenvalues Ω_n with $n \geq 1$ and $\Omega_{n+1} > \Omega_n$, and both the conditional probabilities P_{ij} and their time derivatives \dot{P}_{ij} can be expressed as superpositions of the form $\sum_n C_n \exp(-\Omega_n t)$. Therefore, one has $\dot{P}_{ij}(t) \sim \exp(-\Omega_1 t)$ for large t which also implies $\rho_f(t) \sim \rho_b(t) \sim \exp(-\Omega_1 t)$ via the relations (29) and (30).

Inspection of fig. 5 shows that the decay rate Ω_1 as obtained from our theory is in good agreement with the experimentally observed rate Ω_{ex} for all values of load force and ATP concentration. This agreement is quite remarkable since all transition rates ω_{ij} of the extended (6+2)-network, see table 1, have been obtained in [16] without any reference to the dwell time distributions. Thus, the agreement between theory and experiment as shown in fig. 5 was obtained without any fitting parameter.

Summary. – The mechanical displacement of a molecular motor that walks processively along a filament is governed by four distinct dwell time distributions $\rho_\alpha(t_\alpha)$

for the four co-steps σ_α with $\alpha = \text{ff}$, fb , bf , and bb . These distributions can be obtained from the general relation (13) for the probability distribution of conditional adsorption times. When applied to the network models for kinesin as introduced in [15,16] and displayed in figs. 1 and 2, one obtains the nonexponential dwell time distributions plotted in fig. 4. These distributions for the co-steps determine the dwell time distributions $\rho_f(t_f)$ and $\rho_b(t_b)$ for forward and backward steps via the relations (29) and (30). The tails of these latter distributions are governed by the decay rate Ω_1 , the smallest nonzero eigenvalue of the master equation (4), which is found to be in good agreement with the experimental decay rate Ω_{ex} as obtained in [6], see fig. 5.

This investigation was supported by the EC sixth Framework Program (STREP Contract No. NMP4-CT-2004-516989).

REFERENCES

- [1] HOWARD J., *Mechanics of Motor Proteins and the Cytoskeleton* (Sinauer, New York) 2001.
- [2] SCHLIWA M. and WOEHLKE G., *Nature*, **422** (2003) 759.
- [3] VALE R. D., *Cell*, **112** (2003) 467.
- [4] SVOBODA K., SCHMIDT CH. F., SCHNAPP B. J. and BLOCK ST. M., *Nature*, **365** (1993) 721.
- [5] YILDIZ A., TOMISHIGE M., VALE R. D. and SELVIN P. R., *Science*, **303** (2004) 676.
- [6] CARTER N. J. and CROSS R. A., *Nature*, **435** (2005) 308.
- [7] SCHNITZER M. J. and BLOCK ST. M., *Nature*, **388** (1997) 386.
- [8] HACKNEY D. D., *Proc. Natl. Acad. Sci. U.S.A.*, **102** (2005) 18338.
- [9] GILBERT S. P., MOYER M. L. and JOHNSON K. A., *Biochemistry*, **37** (1998) 792.
- [10] ROMBERG L. and VALE R. D., *Nature*, **361** (1993) 168.
- [11] GUYDOSH N. R. and BLOCK S. M., *Proc. Natl. Acad. Sci. U.S.A.*, **103** (2006) 8054.
- [12] VISSCHER K., SCHNITZER M. J. and BLOCK S. M., *Nature*, **400** (1999) 184.
- [13] SCHNITZER M. J., VISSCHER K. and BLOCK S. M., *Nat. Cell Biol.*, **2** (2000) 718.
- [14] SCHIEF W. R., CLARK R. H., CREVENNA A. H. and HOWARD J., *Proc. Natl. Acad. Sci. U.S.A.*, **101** (2004) 1183.
- [15] LIEPELT S. and LIPOWSKY R., *EPL*, **77** (2007) 50002.
- [16] LIEPELT S. and LIPOWSKY R., *Phys. Rev. Lett.*, **98** (2007) 258102.
- [17] LIPOWSKY R. and LIEPELT S., *J. Stat. Phys.*, **130** (2008) 39.
- [18] LIAO J., SPUDICH J. A., PARKER D. and DELP S. L., *Proc. Natl. Acad. Sci. U.S.A.*, **104** (2007) 3171.
- [19] VAN KAMPEN N. G., *Stochastic Processes in Physics and Chemistry* (Elsevier Science Publisher, Amsterdam) 1992.
- [20] LINDÉN M. and WALLIN M., *Biophys. J.*, **92** (2007) 3804.
- [21] KARLIN S. and TAYLOR H. M., *A First Course in Stochastic Processes* (Academic Press, New York) 1975.